

Using a Microdevice to Generate Alginate Droplets in Sunflower Oil

Letizia Marchetti, Elena Siniscalco, Matteo Antognoli*, Sara Tomasi Masoni, Roberto Mauri, Chiara Galletti, Elisabetta Brunazzi

Dipartimento di Ingegneria Civile e Industriale, Università di Pisa, Largo Lazzarino 2, 56122 Pisa, Italy;
matteo.antognoli@phd.unipi.it

Microfluidic devices may provide significant technological advancement in the production of micro and nanoparticles of interest in the pharmaceutical sector, for instance, particles used as drug carriers (Yeh et al., 2013). Indeed, microfluidics enables their production with precise control of the dimensional distribution, not achievable with conventional beaker methods. The particle size is crucial for the optimal operation, thus representing a key target along with the generation frequency. The device geometry, properties, and flow rates of the fluids are the main parameters that affect the generation process. In this work, we investigate the production of alginate droplets in an X-shaped microdevice (Tomasi Masoni et al., 2022). More specifically, we feed an alginate solution in sunflower oil working in the dripping regime. Experimental visualizations are carried out for different flow rates and concentrations of the surfactant to comprehend their effect on droplet formation. Interestingly, we identify operating conditions that prevent the formation of satellite droplets to preserve a narrow dimensional distribution.

1. Introduction

Engineered particles are widely used in pharmaceutical and medical fields, as they can carry active pharmaceutical ingredients (APIs) and work as scaffold for cell culture or functionalized surfaces for immunoassays. Micro and nanoparticles are mostly used for drug delivery purposes (Sarmiento et al., 2007), thanks to their ability to encapsulate, transport, and controlled-release of APIs in the human body.

Shape, composition, and size determine the quality of particles and chemical or biochemical processes occurring in the compartmentalized volume of fluid. Nanoparticles are divided into spheres and capsules based on shape. Spheres are constituted by a unique homogeneous matrix, while capsules are formed by an external membrane and an internal cavity. Based on raw materials, the particles are classified into organic and inorganic. In the present work, we focus on spherical organic alginate particles. Alginate is a polymeric substance, a linear polysaccharide composed of β -D-mannuronic acid and α -L-glucuronic acid bound with covalent bonds 1-4.

Alginate particles are used for enzyme delivery (Coppi et al., 2002), for the encapsulation of microbes (Kalyanaraman et al., 2009), and for the growth of immobilized *Desmodesmus suspicius* (de Jesus et al., 2019).

Sodium alginate is biodegradable, biocompatible, cheap and easily available, but it may form highly viscous solutions with water, even at low concentrations, which makes it difficult to handle during particle formation. Production methods significantly affect particle quality, especially size, dimensional distribution, and reproducibility, and are divided into batch and microfluidic methods. The batch method includes atomization, coacervation, and emulsification method. They ensure easy equipment and high productivity, but with poor control of the particle dimension; indeed, it usually requires an additional filtration step to select the target-sized particles. The microfluidic method allows better control of the size distribution, as a microfluidic device generally treats low flow rates of liquid fluids in a small volume. Although this leads to less productivity with respect to the batch method the numbering-up method, i.e., placing several devices in parallel, can overcome the limit and avoid the scale-up procedure. Moreover, the microfluidic approach is a sustainable choice that ensures savings

on energy consumption and quantity of reagent, with a smaller amount of waste. For all these reasons, the microfluidic method has been widely adopted for making particles during the last decade.

The microfluidic method includes two techniques to produce droplets, i.e., solvent displacement and segmentation. The solvent displacement technique considers two phases: the solvent contains the raw material of the particles, and the antisolvent is made with a substance in which the solvent can be dissolved but the raw material cannot. In this way, when the two phases are fed into the microdevice, the generation of the drops occurs thanks to the transfer of the solvent and the variation of the concentration. The segmentation or pinching method considers two immiscible phases, i.e., continuous and dispersed phases. When the two phases come into contact in the confluence region two main forces arise: the destabilizing one, as the interfacial force, promote the formation of the droplet, instead the stabilizing forces, as inertial and viscous forces favour the jet extension. The ratio between these forces influences the flow features, leading to the different flow regimes in the microdevice: the dripping, squeezing, and jetting regime. In the dripping regime, the droplet is formed in the confluence region, with a characteristic size smaller than that of the microchannels. In the squeezing regime, the droplet size is bigger than the characteristic size of microchannels. Instead, the jetting regime provides the droplet formation downstream of the jet extension. Hence, a suitable regime for making engineered particles is the dripping flow, as it ensures better control over the size of the droplets and narrow size distribution. The segmentation method can be applied to form uniform droplets of sodium alginate, that can be jellified in a batch of calcium chloride in a second phase (Chan et al., 2009).

Therefore, this work aims to investigate the microfluidic production of alginate droplets with the pinching technique in an X-shaped microdevice presenting square cross-section. The channel characteristic size is 1 mm to allow us to test the production of microparticles using a highly viscous sodium alginate solution and reduce the chance of channel clogging. The operating conditions are spanned to optimize the droplet formation process.

2. Experimental Setup

Figure 1 shows the X-shaped microdevice, which consists of four identical channels in a flow-focusing configuration, i.e., three inlets and one outlet, with a square cross-section of 1 mm x 1 mm. The length of the channels is 60 mm. The microdevice is made with three layers of polymethylmethacrylate (PMMA), which are sealed with two double-sided (Nitto-Denko, 597A-597AP) adhesive films, having an overall thickness equal to 50 μm before being tightened with screws. The central layer, which is 1 mm thick, has an X-shape cut, while the top and bottom layers have a thickness of 3 mm each.

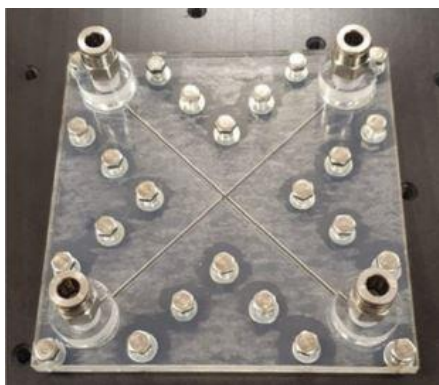


Figure 1 Picture of the fabricated PMMA X-shaped microdevice for the experiments.

One of the inlet channels is fed with an aqueous solution of alginate, which is the dispersed phase, and the other two opposite channels are fed with the continuous phase. The dispersed phase is prepared by dissolving sodium alginate (CAS No. 9005-38-3, Sigma Aldrich, Steinheim, Germany) in deionized water, with a concentration of 2 wt%. To single out the effect of the surfactant, two different continuous phases are prepared: the first one is made of sunflower oil and 0.5 wt% of Span 80 (CAS No. 1338-43-8, Sigma Aldrich, St. Louis, USA) and the second one is made only of sunflower oil. The surface tension between the two phases is measured with a ring tensiometer finding that the Span 80 surfactant can significantly decrease the surface tension from 0.038 N·m to 0.020 N·m. Density and viscosity are not affected by the addition of the surfactant. The physical properties of the two solutions are summarized in Table 1. The density is obtained from the literature (Del Gaudio P. et al., 2005); instead, the viscosity is directly measured with the Ubbelohde viscosimeter by averaging the resulting values achieved from three experiments.

Table 1 Physical properties of the working fluids (the reference temperature is 25°C).

	Density [kg/m ³]	Viscosity [mPa · s]
Dispersed phase	1003.2	241.2
Continuous phases	913.3	79.5

The experimental setup is represented in Figure 2. The continuous phase is introduced by using a KD Scientific syringe pump Gemini 88 and the dispersed phase is fed with a Harvard Apparatus syringe pump, equipped with two Becton Dickson luer-lock plastic syringes of 20 mL and one of 5 mL, respectively. The PVC tubes have a diameter of 2 mm and a thickness of 1 mm.

Experiments are carried out in a controlled-temperature room at 25 °C.

The flow inside the microdevice is observed using an upright microscope model Nikon Eclipse 80i equipped with a magnifying lens of 4× having an aperture value equal to $N.A. = 0.13$. The light source is an OSRAM Xenophon FCR 64625 HLX 12 V-100 W) lamp. Experimental images are acquired with the high-speed camera Optomotive Velociraptor HS, which has a square monochrome sensor with a resolution of 2048 × 2048 pixels and the maximum frame rate is 174 frames/s for the whole sensor. Furthermore, all the experiments are performed in a dark room to maintain a constant level of luminosity and to minimize any reflection and shadow.

The alginate solution is coloured by adding a negligible quantity of red dye (E124) improving the contrast between the dispersed and continuous phases. At least 200 images with size 500×2048 are collected for each test, tuning the frame rate acquisition depending on the flow rate. The maximum frame rate employed is 100 Hz, which is sufficient to capture several instants of the pinching process.

At the end of each experiment, the device and tubes are cleansed from the sodium alginate solution with deionized water twice: the first time with a rapid wash (pushing the syringes by hand) and then at a low flow rate for an overnight wash (18 hours).

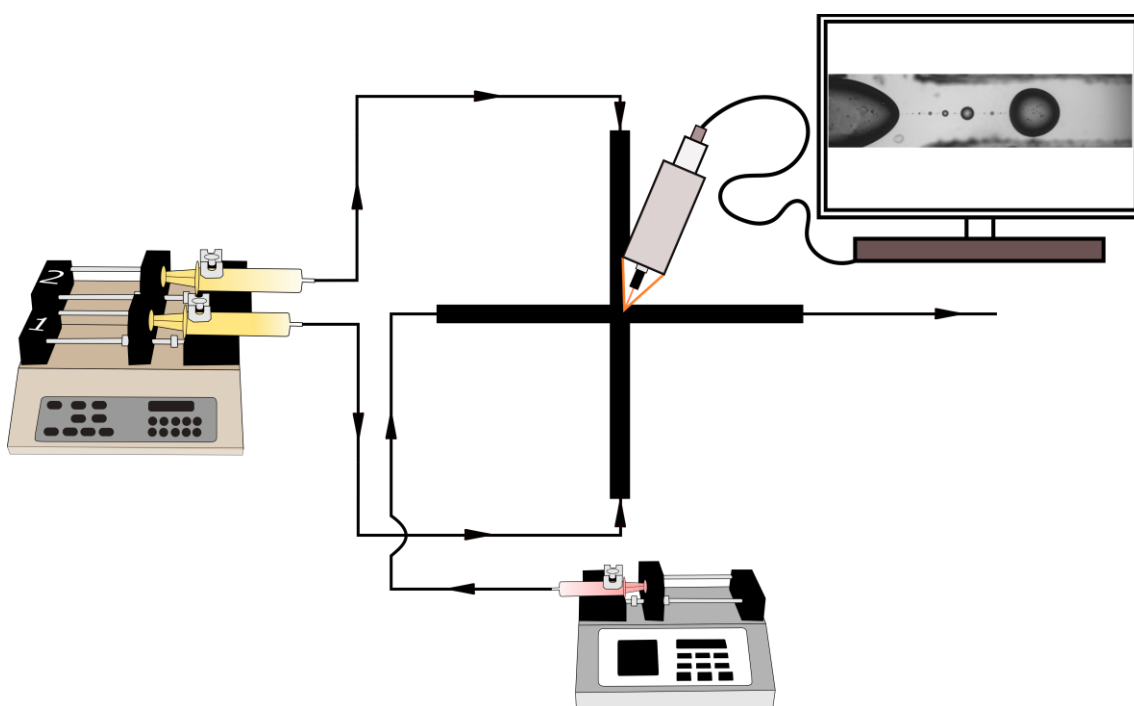


Figure 2 Schematic representation of the experimental setup, consisting of two syringe pumps, a microscope and a high-speed camera.

3. Results

This section describes the main experimental results focusing on the role of surfactant and then of the flow rates in the pinching process working in dripping flow conditions.

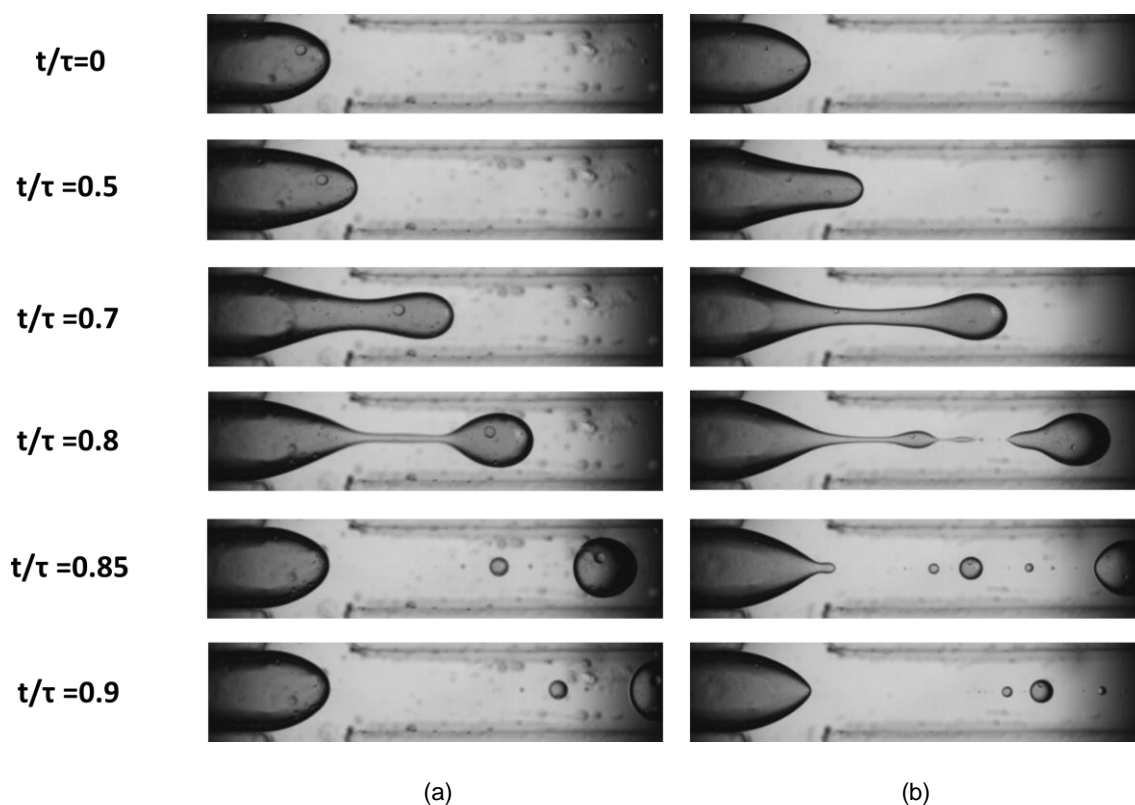


Figure 3 Pinching process (a) in the presence and (b) absence of Span 80 surfactant. The continuous phase flow rate is equal to 400 $\mu\text{L}/\text{min}$ and the dispersed phase flow rate is 10 $\mu\text{L}/\text{min}$.

Figure 3 shows the alginate droplet generation obtained in presence of the Span 80 surfactant in the continuous phase (Figure 3a) and without it (Figure 3b), feeding 400 $\mu\text{L}/\text{min}$ of the oil phase and 10 $\mu\text{L}/\text{min}$ of the aqueous one. After a few seconds of transient flow, the dynamic process becomes cyclic. Both figures contain six experimental images obtained at different instants of the cycle. The instants are made dimensionless with respect to the cycle period τ . From $t/\tau = 0$ to $t/\tau = 0.5$, the alginate phase stretches into the outlet channels. Then, a striction in the aqueous solution is formed and becomes thinner until $t/\tau = 0.8$, when the droplet detaches from the inlet streams. This instant is critical, as it determines the size of the main droplet as well as the formation of satellite droplets. Afterwards, the droplets are driven downstream in the outlet channel.

The satellites are not desirable, because it is possible to control neither their shape nor their dimensions.

Comparing Figure 3a and b, it is worth mentioning that fewer satellites are formed using the surfactant. Furthermore, in Figure 3b, the droplet forms further downstream in the outlet channel. Therefore, the use of surfactant seems to facilitate the pinching of the dispersed phase achieving a neater cut of the fluid. On the other hand, the presence of surfactant may be undesirable, as it can inhibit or alter chemical or biochemical reactions in the application of interest. For such a reason, the Span 80 concentration was limited to 0.5 wt% in this investigation.

The surfactant promotes the formation of more uniform droplets; thus, the pinching process is now observed by varying the inlet flow rates in presence of the Span 80 surfactant.

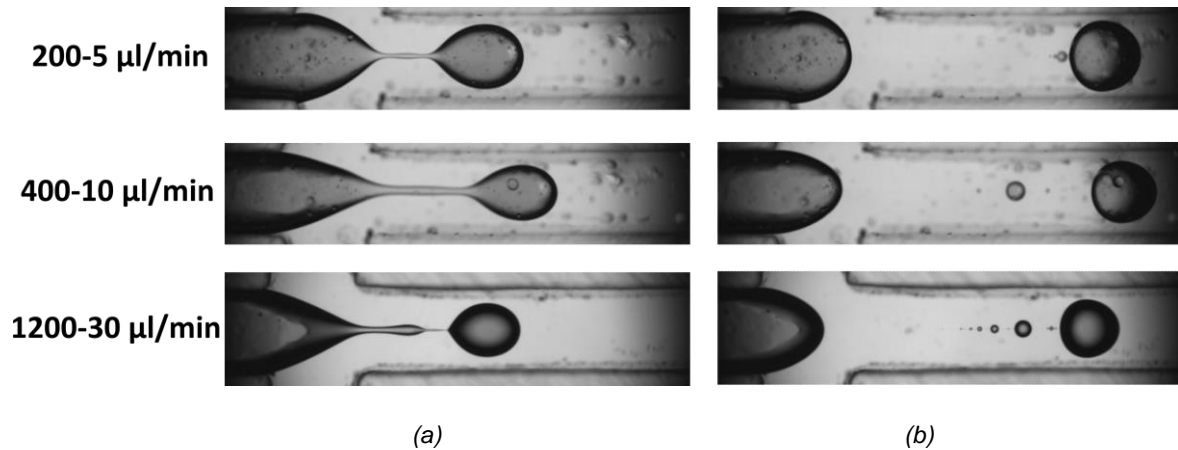


Figure 4 Comparison between different inlet flow rates, keeping the ratio between the flow rate equal to 40, of the pinching process at instants (a) $t/\tau = 0.8$ and (b) $t/\tau = 0.85$.

Figure 4 shows a comparison between the droplets obtained with different inlet flow rates. In the figure, the flow rates increase from top to bottom. Two different instants are shown in Figure 4: on the left, a moment before the pinching phase, and on the right, an instant later. In the former, it appears that more fluid is retained behind the main droplet by increasing the inlet flow rates. The latter shows the diameter of the droplet shrinks with the increase of the fluid velocity, and both the dimensions and the number of satellites grow up.

To quantify the presence of undesirable satellite droplets, an automated MATLAB® code is created to evaluate the pinching efficiency and the droplet diameters.

The routine examines several images at the instant $t/\tau = 0.85$ from the collected experimental frames. The images are post-processed to represent and analyze the region occupied only by the dispersed phase, as depicted in Figure 5.

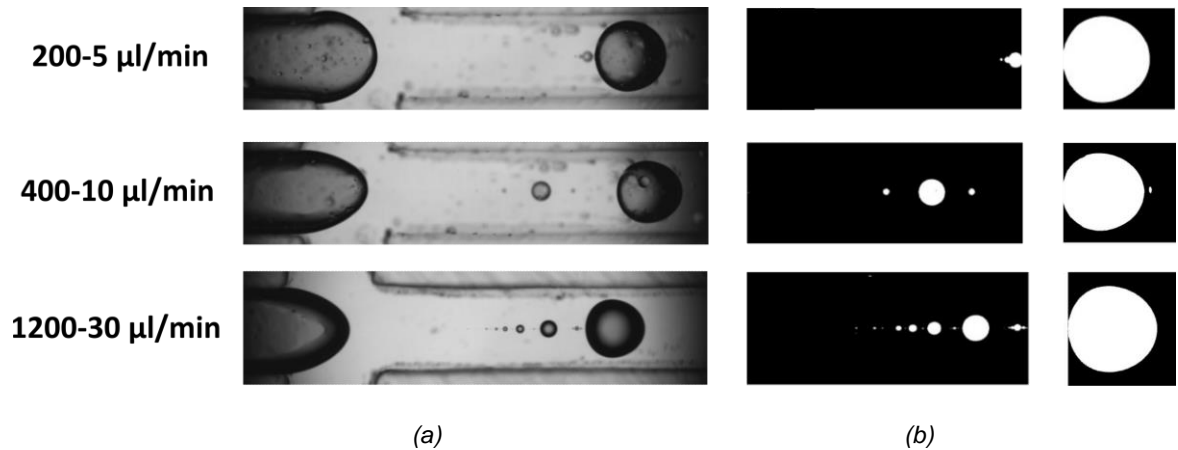


Figure 5 (a) Experimental frames and (b) zoom of the post-processed images obtained with MATLAB®: the white regions indicate the extension of the dispersed phase occupied by the satellite droplets and the main one.

Eventually, the droplet diameters are evaluated by assuming perfectly spherical-shaped droplets. We define the pinching efficiency (φ) as the ratio between the volume occupied by the main droplet and the total volume of the dispersed phase:

$$\varphi = \frac{V_1}{V_2 + V_1}$$

where V_1 is the volume of the main droplet and V_2 is the volume of satellite droplets. It is worth noting that the product of the pinching efficiency with the flow rate of the dispersed phase represents the portion of the volumetric flow rate used to form the main droplet.

Accordingly, it is possible to calculate the diameter of the main droplets for each operating condition analyzed.

Table 2 Pinching efficiency and main droplet diameter for different inlet flow rates.

Continuous flow rate [$\mu\text{L}/\text{min}$]	Dispersed flow rate [$\mu\text{L}/\text{min}$]	φ [%]	Productivity [$\mu\text{L}/\text{min}$]	Diameter [mm]
200	5	99.33	4.81	0.86
400	10	96.53	9.65	0.80
1200	30	95.43	28.6	0.76

Table 2 shows the experimental diameter of the main droplet and pinching efficiency for the three flow combinations. Both the efficiency and the droplet diameter decrease as the flow rates increase. Thus, by increasing the flow rates there is an increase in productivity and the generation of dispersion of drops with smaller diameters, however at the expense of a greater number of satellites. Indeed, we consider the productivity as the product of pinching efficiency and volumetric flow rate of alginate solution, which denotes the alginate solution volume that has effectively encapsulated into the main droplet, excluding any contribution of the satellite droplets.

4. Conclusions

The present work has investigated the segmentation process in an X-shaped microfluidic device by using sunflower oil and a highly viscous solution of sodium alginate. The physical and interfacial properties of the two phases have been observed in the presence and absence of surfactant. The surfactant significantly affects the pinching process during droplet generation, promoting the formation of more uniform droplets and, thus, microparticles. In addition, the investigation has spanned different inlet flow rates at the same flow rate ratio between the dispersed and continuous phases. The results have shown that by increasing the flow rates it is possible to generate smaller particles with a broader diameter distribution. Based on the available data, the case of 400 $\mu\text{L}/\text{min}$ of the oil phase and 10 $\mu\text{L}/\text{min}$ of the aqueous one could represent a tradeoff between pinching efficiency and droplet productivity. The developed MATLAB[®] code, which allows to evaluate the pinching efficiency based on the relevance of undesirable satellites, could be a useful tool to control the pinching process and the droplet quality in microfluidic devices. Further studies and additional experimental data are required spanning the inlet flow rates at different flow rate ratios. These data may represent a useful validation dataset for the implementation of more advanced numerical methods, such as multiphase Computational Fluid Dynamics. Indeed, numerical modelling could provide further insights into the pinching process and the optimal working conditions, also exploiting numerical sensitivity analysis tools.

References

- Chan E.S., Lee B. B., Ravindra P., Poncelet D., 2009, Prediction models for shape and size of calcium-alginate macrobeads produced through extrusion-dripping method, *Journal of Colloid and Interface Science*, 338 (1), pp. 63 - 72
- Coppi G., Iannuccelli V., Bernabei M.T., Cameroni R., 2002, Alginate microparticles for enzyme peroral administration, *International Journal of Pharmaceutics*, 242 (1-2), pp. 263 - 266
- de Jesus G.C., Gaspar Bastos R., Altenhofen da Silva M., 2019, Production and characterization of alginate beads for growth of immobilized *Desmodesmus subspicatus* and its potential to remove potassium, carbon and nitrogen from sugarcane vinasse, *Biocatalysis and Agricultural Biotechnology*, 22, art. no. 101438
- Del Gaudio P., Colombo P., Colombo G., Russo P., Sonvico F., 2005, Mechanisms of formation and disintegration of alginate beads obtained by prilling, *International Journal of Pharmaceutics*, 302 (1-2), pp. 1 - 9
- Kalyanaraman M., Retterer S.T., McKnight T.E., Ericson M.N., Allman S.L., Elkins J.G., Palumbo A.V., Keller M., Doktycz M.J., 2009, Controlled microfluidic production of alginate beads for in situ encapsulation of microbes, 1st Annual ORNL Biomedical Science and Engineering Conference, BSEC 2009, art. no. 5090482
- Sarmento B., Ribeiro A., Veiga F., Sampaio P., Neufeld R., Ferreira D., 2007, Alginate/chitosan nanoparticles are effective for oral insulin delivery, *Pharmaceutical Research*, 24 (12), pp. 2198 - 2206
- Tomasi Masoni S., Antognoli M., Mariotti A., Mauri R., Salvetti M.V., Galletti C., Brunazzi E., 2022, Flow regimes, mixing and reaction yield of a mixture in an X-microreactor, *Chemical Engineering Journal*, 437, art. no. 135113
- Yeh C.H., Zhao Q., Lee S.J., Lin Y.C., 2009, Using a T-junction microfluidic chip for monodisperse calcium alginate microparticles and encapsulation of nanoparticles, *Sensors and Actuators, A: Physical*, 151 (2), pp. 231 - 236